Electronic Supplementary Information (ESI) for *Dalton Transactions*

Single-Molecule Magnet Behaviour in a Centrosymmetric Dinuclear Dysprosium(III) Complex: Sequential Distinguish of Triple Relaxation Pathways

Xiao-Jiao Song,[a,b] Yu Jing,[a] Xin Feng,[a] Zhao-Bo Hu,*[c] Ming Kong,[a] Xiao-Ming Xue,[b] Yi-Quan Zhang*[d] and You Song*[a]

[a] State Key Laboratory of Coordination Chemistry, School of Chemistry and Chemical Engineering, Nanjing University, Nanjing 210023, P. R. China

[b] Key Laboratory of National Forestry and Grassland Administration on Wildlife Evidence Technology, School of Criminal Science and Technology, Nanjing Forest Police College, Nanjing 210023, P. R. China

[c] Chaotic Matter Science Research Center, Department of Materials, Metallurgy and Chemistry, Jiangxi University of Science and Technology, Ganzhou 341000, P. R. China

[d] Jiangsu Key Lab for NSLSCS, School of Physical Science and Technology, Nanjing Normal University, Nanjing 210023, P. R. China

*** Correspondence:**
Corresponding Author: Zhao-Bo Hu, Yi-Quan Zhang, You Song
e-mail: *huzhaobo@smail.nju.edu.cn, *zhangyiquan@njnu.edu.cn, *yousong@nju.edu.cn

Physical Measurements

Elemental analyses of C, H and N were carried out with a PerkinElmer 240C elemental analyzer. The ratio of Dy/Y was determined with XRF (EDAX Orbis).The IR spectra were recorded with a Nicolet iS10 spectrometer using KBr pellets in the range 400-4000 cm^{-1}. Powder X-ray diffraction (PXRD) were measured on a Bruker AXS D8 Advance powder diffractometer (Cu-Kα, λ = 1.54056 Å), with a scan speed of 0.5 s/step and a step size of 0.01° in 2θ. Data of magnetic properties for crystalline sample were collected on a Quantum Design MPMP-XL 7 superconducting quantum interference device (SQUID) magnetometer and a Quantum Design MPMS SQUID-VSM.

Table S1 Crystallographic data and structural refinement parameters for **Dy_2**.

	Dy_2
Formula	$C_{52}H_{56}Cl_2Dy_2N_6O_8$
f w	1288.93
T / K	296(2)
λ / Å	0.71073
Crystal system	Monoclinic
Space group	$P2_1/c$
a / Å	13.122(4)
b / Å	10.371(3)
c / Å	19.538(6)
α / º	90
β / º	103.71(3)
γ / º	90
V / $Å^3$	2585.5(13)
Z	2
D_c / g cm^{-3}	1.656
μ / mm^{-1}	3.030
F(000)	1280.0
θ / °	2.144~27.594
Reflns collected, Reflns unique	21796, 5934
R_{int}	0.0671
GOF on F^2	1.028
R_1 [I> 2σ(I)][a], R_1 (all data)[a]	0.0437, 0.0499
wR_2 [I>2σ(I))][b], wR_2 (all data)[b]	0.1288,0.1301
Largest diff. Peak, hole / (e $Å^{-3}$)	1.286, -1.801

[a]$R_1 = \Sigma$ ||Fo| – |Fc||/Σ|Fo|; [b]$wR_2 = [\Sigma w(Fo^2 - Fc^2)^2/\Sigma w(Fo^2)^2]^{½}$

Table S2 Selected bond lengths (Å) and angles (°) for **Dy_2**.

Bond lengths around Dy1			
Dy1-O1	2.190(3)	Dy1-O2	2.239(3)
Dy1-O3	2.398(3)	Dy1-O4	2.240(3)
Dy1-N1	2.492(4)	Dy1-N2	2.504(3)
Dy1-Cl1	2.681(11)		
Bond angles including Dy1			
O1-Dy1-O2	144.96(12)	O1-Dy1-O3	76.61(13)
O1-Dy1-O4	86.74(13)	O2-Dy1-O3	71.87(12)
O2-Dy1-O4	81.03(12)	O4-Dy1-O3	94.69(13)
O1-Dy1-N1	72.61(13)	O2-Dy1-N1	141.55(12)
O3-Dy1-N1	145.56(12)	O4-Dy1-N1	98.57(12)
O1-Dy1-N2	136.29(13)	O2-Dy1-N2	73.83(12)
O3-Dy1-N2	145.69(12)	O4-Dy1-N2	80.67(12)
N1-Dy1-N2	68.25(12)	O1-Dy1-Cl1	105.26(10)
O2-Dy1-Cl1	90.24(9)	O3-Dy1-Cl1	90.74(10)
O4-Dy1-Cl1	167.72(9)	N1-Dy1-Cl1	82.88(9)
N2-Dy1-Cl1	88.63(8)		

Table S3 Deviation parameters calculated by SHAPE for seven-coordinated Dy (III) center in **Dy_2**. The best match is displayed in bold with blue color.

Geometry	Point group	Polyhedron	Dy1
HP-7	D_{7h}	Heptagon	22.876
HPY-7	C_{6v}	Hexagonal pyramid	19.259
PBPY-7	D_{5h}	Pentagonal bipyramid	6.894
COC-7	C_{3v}	Capped octahedron	11.038
CTPR-7	C_{2v}	Capped trigonal prism	8.146
JPBPY-7	***D_{5h}***	**Johnson pentagonal bipyramid (J13)**	**4.180**
JETPY-7	C_{3v}	Elongated triangular pyramid (J7)	17.210

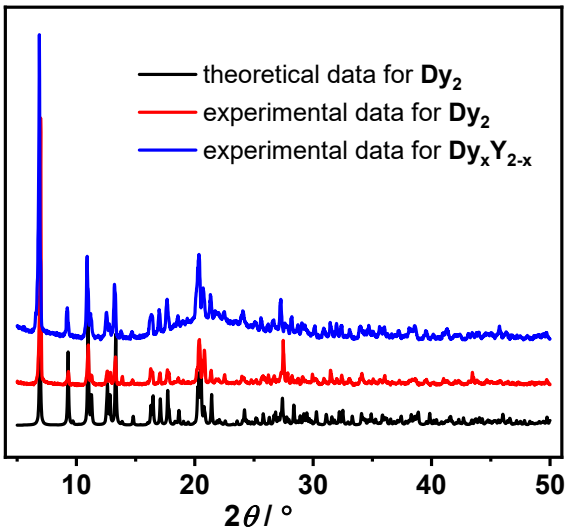

Fig. S1 The theoretical X-ray powder diffraction patterns (black), the experimental ones of $\mathbf{Dy_2}$ (red) and $\mathbf{Dy_xY_{2-x}}$ (blue).

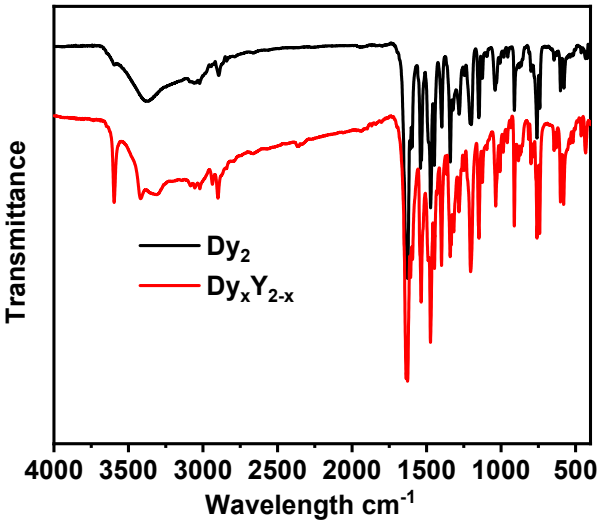

Fig. S2 The FT-IR spectra of $\mathbf{Dy_2}$ (black) and $\mathbf{Dy_xY_{2-x}}$ (red).

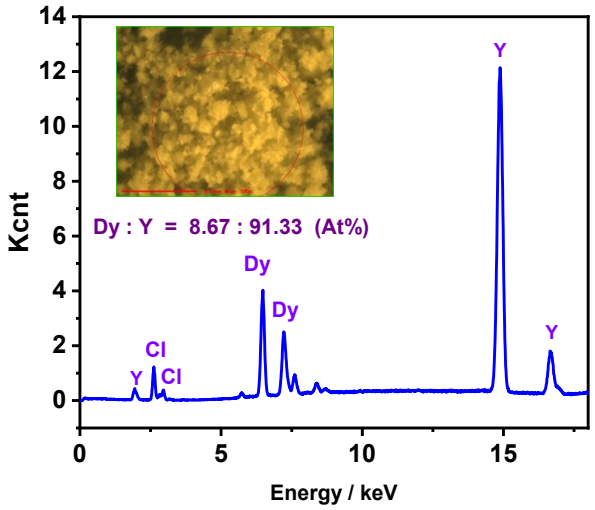

Fig. S3 Energy spectrum of $\mathbf{Dy_xY_{2-x}}$.

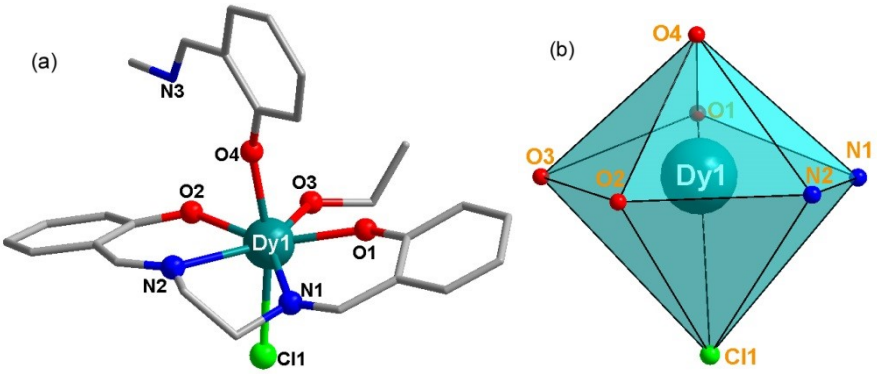

Fig. S4 (a) Perspective view of the asymmetric unit of $\mathbf{Dy_2}$, (b) the coordination geometry of Dy(III) ion in $\mathbf{Dy_2}$.

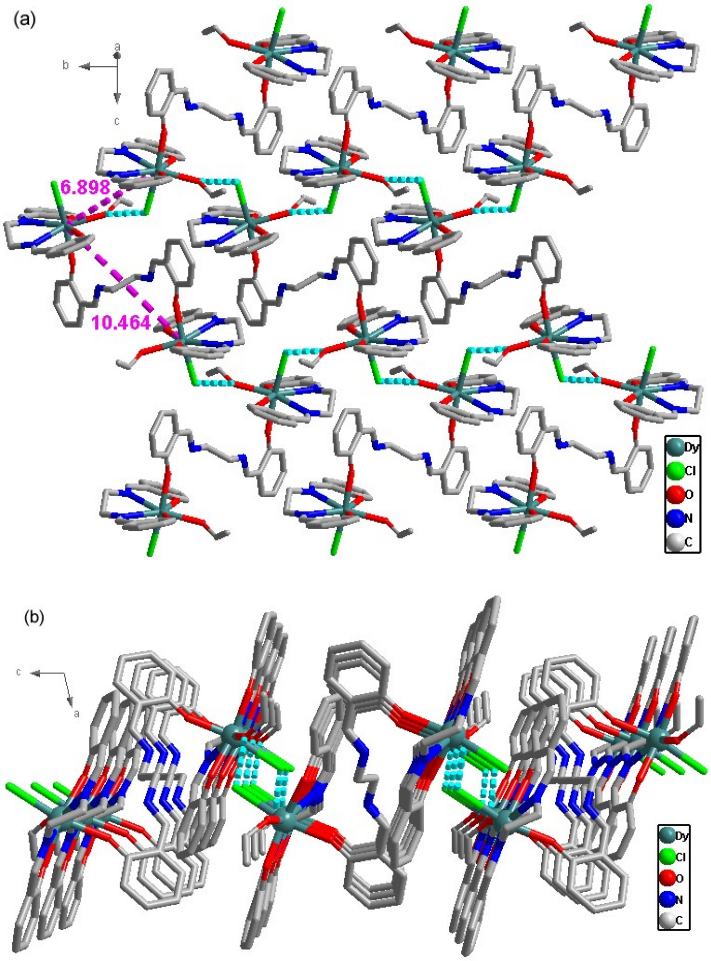

Fig. S5 (a) The 2D network of $\mathbf{Dy_2}$ in the *bc* plane formed via hydrogen bonds, the shortest interdimer Dy···Dy separation is 6.898 Å, while the Dy···Dy distance within the dinuclear molecule is 10.464 Å. (b) View of the network along the b direction.

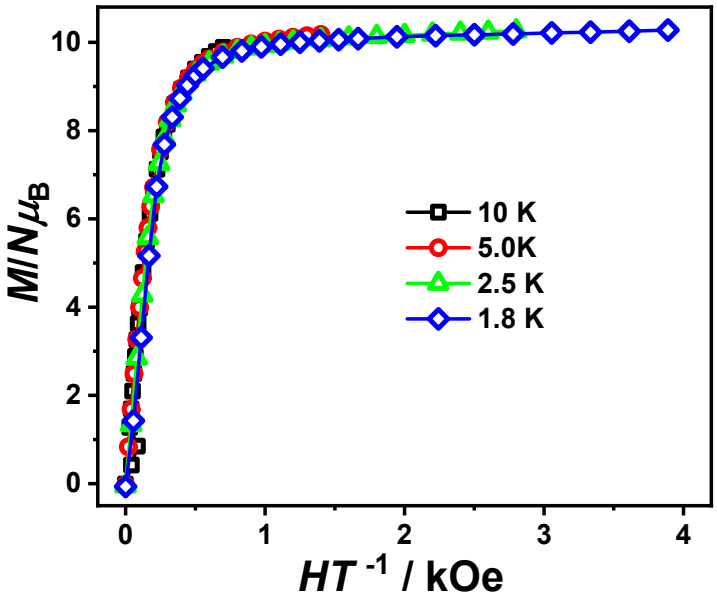

Fig. S6 Plots of *M* vs *H* / *T* for **Dy$_2$** at 1.8, 2.5, 5.0 and 10 K.

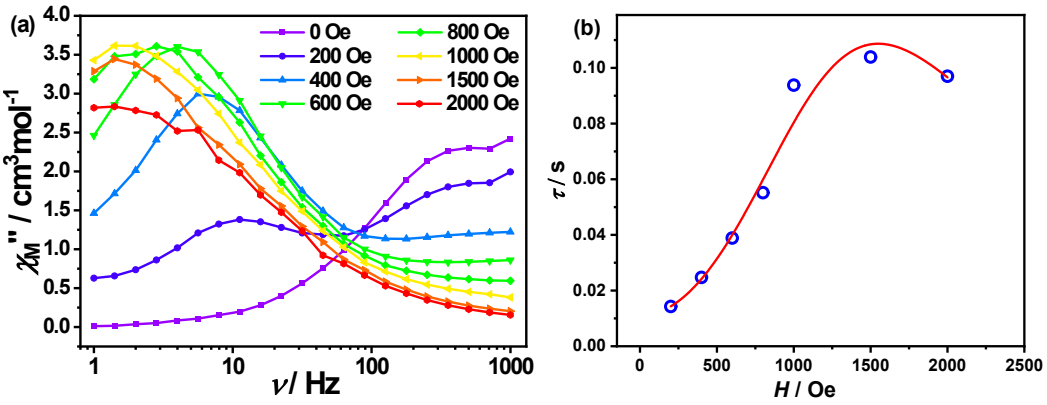

Fig. S7 (a) χ''_M vs. ν plot at 1.8 K in the frequency range of 1-1000 Hz under various applied dc field for **Dy$_2$**. (b) Field-dependence of the relaxation time (blue circles) and the best fit curve (red line) for **Dy$_2$**.

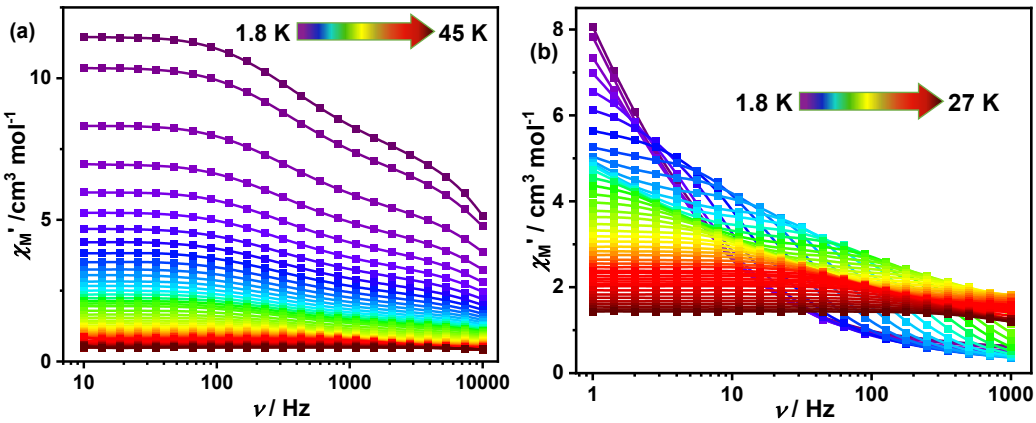

Fig. S8 Frequency-dependent of in-put phase (χ_M') ac susceptibilities under zero field (a) and under 1.5 kOe dc field (b) for **Dy$_2$**.

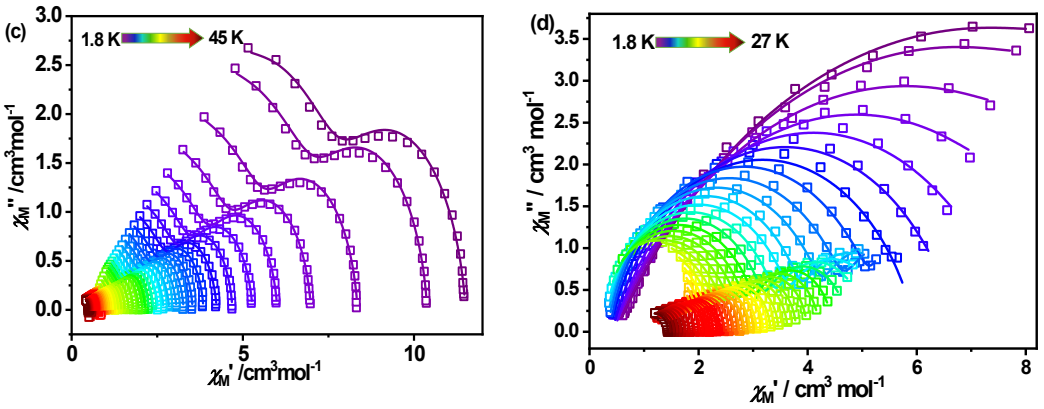

Fig. S9 Cole-Cole curves under zero dc-field (a) and under 1.5 kOe (b) for **Dy_2**. Solid lines represent the best fit with extended Debye model.

Table S4 The best-fitted parameters obtained from the analyses of the Cole-Cole plots using the extended Debye model for **Dy_2** under zero field.

T / K	χ_S(total) / cm^3 mol^{-1}	$\Delta\chi_1$ / cm^3 mol^{-1}	ln(τ_1 / s)	α_1	$\Delta\chi_2$ / cm^3 mol^{-1}	ln(τ_2 / s)	α_2	R^2
1.8	2.22637	3.80538	-7.42174	0.11629	5.47416	-11.5272	0.07449	0.07321
2	1.13894	3.25038	-7.409	0.10128	5.99599	-11.5615	0.15906	0.06844
2.5	0.45584	2.59914	-7.42457	0.09735	5.2956	-11.6221	0.198	0.04594
3	0.17147	2.22266	-7.42598	0.10622	4.59887	-11.6721	0.20965	0.01969
3.5	2.50E-13	1.91166	-7.43447	0.10409	4.09645	-11.6985	0.22325	0.01399
4	4.03E-13	1.73023	-7.43589	0.11549	3.55491	-11.7209	0.21778	0.00876
4.5	3.18E-13	1.51608	-7.42881	0.10107	3.18424	-11.7432	0.22587	0.01841
5	4.76E-13	1.38504	-7.42881	0.10601	2.85336	-11.7676	0.22376	0.01053
5.5	8.00E-13	1.25263	-7.43872	0.09946	2.6016	-11.7852	0.22811	0.01148
6	5.63E-13	1.15394	-7.45287	0.09966	2.38418	-11.8098	0.23028	0.01086
6.5	5.36E-13	1.07261	-7.45146	0.10002	2.19978	-11.8368	0.2318	0.00945
7	4.95E-13	1.04319	-7.46561	0.12073	2.02294	-11.8792	0.2257	0.00591
7.5	7.93E-13	0.95838	-7.47976	0.11172	1.89248	-11.9005	0.22831	0.00439
8	9.95E-13	0.91098	-7.48725	0.11444	1.77641	-11.9292	0.23196	0.00559
8.5	1.69E-12	0.84579	-7.50699	0.1053	1.67595	-11.9523	0.23446	0.00533
9	2.75E-12	0.80939	-7.51885	0.1088	1.57898	-11.9842	0.23232	0.00299
9.5	3.66E-12	0.74331	-7.52956	0.08875	1.5114	-12	0.24336	0.00477
10	4.44E-12	0.70457	-7.54317	0.08202	1.44073	-12.0287	0.24741	0.00451
10.5	5.88E-12	0.69677	-7.57034	0.09603	1.36304	-12.0747	0.2421	0.00391
11	7.85E-12	0.66175	-7.60147	0.08963	1.30203	-12.1104	0.24295	0.00333
12	9.47E-12	0.60665	-7.6595	0.07873	1.19521	-12.1976	0.24612	0.00266
13	1.21E-11	0.56731	-7.73733	0.07241	1.09943	-12.3181	0.24506	0.00177
14	1.19E-11	0.52959	-7.81269	0.06139	1.02078	-12.4788	0.25346	0.0016
15	1.99E-11	0.50009	-7.92391	0.05417	0.94864	-12.6912	0.26223	7.81E-04
16	4.89E-11	0.46112	-8.03778	0.03379	0.89577	-12.9619	0.29817	0.00113
17	1.37E-10	0.43076	-8.17381	0.01799	0.84303	-13.2756	0.32504	0.00134

18	3.49E-10	0.41806	-8.29907	0.02009	0.79222	-13.6765	0.35456	9.57E-04
19	2.42E-21	0.40083	-8.42318	0.02151	0.75101	-14.1635	0.40614	4.11E-04
20	4.53E-21	0.39783	-8.5713	0.02965	0.69702	-14.5082	0.37879	3.99E-04
21	3.29E-21	0.37924	-8.70915	0.02037	0.66084	-14.8249	0.38394	3.16E-04
22	2.11E-21	0.37639	-8.83329	0.03263	0.62199	-15.2084	0.37363	2.43E-04
23	4.70E-21	0.36885	-8.9569	0.03569	0.58924	-15.4957	0.35317	2.71E-04
24	7.80E-21	0.34786	-9.07716	0.02177	0.56659	-15.5789	0.35078	1.24E-04
25	1.09E-20	0.33591	-9.18958	0.01211	0.54174	-15.2541	0.25318	0.00312
26	2.74E-20	0.32294	-9.30111	0.00757	0.52011	-15.1956	0.21078	0.00141
27	2.81E-20	0.31329	-9.40996	0.00858	0.49982	-15.3115	0.18999	0.0037
28	5.55E-23	0.31469	-9.52568	0.03305	0.4762	-17.1733	0.34232	0.01051
29	5.24E-23	0.28839	-9.64753	2.78E-15	0.46561	-16.9374	0.35154	0.0047
30	1.09E-22	0.28098	-9.75779	1.36E-14	0.44765	-14.8999	3.27E-08	0.00851
31	1.03E-22	0.27572	-9.81616	1.66E-14	0.43687	-14.9739	4.66E-08	0.00194
32	8.86E-23	0.26685	-9.91949	2.12E-14	0.42139	-15.1071	6.89E-08	0.00137
33	8.85E-23	0.2591	-10.0283	2.67E-14	0.40802	-15.2011	9.62E-08	0.00466
34	9.20E-23	0.25326	-10.1088	3.33E-14	0.39802	-15.3229	1.35E-07	0.00218
35	8.75E-23	0.24621	-10.2226	4.27E-14	0.38526	-15.4921	1.90E-07	0.00479
36	9.21E-23	0.24048	-10.3122	6.34E-14	0.3757	-15.6548	1.65E-07	0.00219
37	9.93E-23	0.23411	-10.4311	8.91E-14	0.36367	-15.7877	1.75E-07	0.00197
38	1.16E-22	0.22789	-10.5376	1.12E-13	0.35416	-15.8257	1.79E-07	0.00659
39	1.40E-22	0.22371	-10.6709	1.59E-13	0.34148	-16.2156	2.89E-07	0.00321
40	3.11E-22	0.21692	-10.7653	1.14E-13	0.33562	-15.862	3.77E-08	0.00972
41	3.43E-22	0.21164	-10.8811	1.52E-13	0.32769	-15.8822	3.72E-08	0.00556
42	1.13E-22	0.20372	-10.9449	2.48E-13	0.32694	-15.9893	5.24E-08	0.00523
43	1.55E-22	0.20589	-11.1451	3.02E-13	0.30818	-16.6812	7.29E-08	0.00286
44	1.80E-23	0.19322	-11.1967	4.17E-18	0.3132	-15.9567	1.84E-07	0.00374
45	3.38E-23	0.1953	-11.3805	4.69E-18	0.29838	-16.7962	1.80E-07	0.00165

$\chi_{T1} = \chi_S(\text{Total}) + \Delta\chi_1$, $\chi_{T2} = \chi_S(\text{Total}) + \Delta\chi_1 + \Delta\chi_2$

Table S5 The best-fitted parameters obtained from the analyses of the Cole-Cole plots using the extended Debye model for **Dy_2** under 1.5 kOe dc field.

T / K	χ_S(Total)/ cm^3 mol^{-1}	$\Delta\chi_1$ / cm^3 mol^{-1}	ln(τ / s)	α	$\Delta\chi_2$ / cm^3 mol^{-1}	ln(τ / s)	α	R^2
5	0.36662	4.8601	-5.02426	0.13191	3.52078	-0.63583	9.53E-08	0.03767
5.5	0.33193	4.38866	-5.49088	0.1132	2.00161	-1.0561	1.99E-07	0.01872
6	0.30277	3.99807	-5.92808	0.09455	1.88567	-1.51264	6.01E-09	0.01153
6.5	0.296	3.62183	-6.34813	0.06942	1.78394	-1.94292	1.54E-08	0.02245
7	2.61E-01	3.42518	-6.69349	0.07508	1.64951	-2.26477	2.44E-08	0.0045
7.5	2.44E-01	3.18631	-7.03614	0.06837	1.58686	-2.59206	4.08E-08	0.00675
8	2.41E-01	2.97446	-7.3542	0.05881	1.49704	-2.90742	7.53E-08	0.00453
8.5	2.09E-01	2.83282	-7.65622	0.06478	1.40192	-3.19793	5.18E-08	0.00522
9	1.88E-01	2.68717	-7.94628	0.06695	1.32934	-3.47028	9.84E-08	0.00286

9.5	1.79E-01	2.55793	-8.2171	0.07011	1.25156	-3.73246	9.84E-08	0.00501
10	1.18E-01	2.48201	-8.51553	0.07987	1.18839	-4.02019	2.67E-07	0.00568
10.5	3.70E-02	2.44629	-8.81349	0.09069	1.14561	-4.23403	3.71E-07	0.00522
11	4.63E-15	2.36845	-9.09656	0.09122	1.09348	-4.50292	7.57E-07	0.00269
11.5	5.59E-15	2.25969	-9.35168	0.08363	1.05445	-4.73458	1.09E-06	0.00338
12	7.54E-15	2.16445	-9.60883	0.07811	1.01562	-4.95203	2.11E-06	0.00445
12.5	1.23E-14	2.07588	-9.83641	0.07544	0.98309	-5.15482	2.10E-06	0.0031
13	1.49E-14	1.99539	-10.0972	0.07416	0.94162	-5.36982	3.03E-06	0.00194
13.5	1.75E-14	1.92276	-10.3415	0.07171	0.90679	-5.57001	4.25E-06	0.00261
14	2.55E-15	1.85255	-10.626	0.07862	0.88655	-5.76185	8.19E-06	0.00332
14.5	3.74E-15	1.78503	-10.8432	0.06602	0.85311	-5.9344	1.09E-05	0.00138
15	3.41E-15	1.73706	-11.2378	0.12766	0.80946	-6.09631	1.70E-05	0.00132
15.5	3.80E-15	1.68747	-11.7475	0.18558	0.78439	-6.2509	2.17E-05	6.53E-04
16	3.25E-15	1.64433	-12.6346	0.31895	0.74256	-6.40693	3.21E-05	0.00163
16.5	2.22E-15	1.60272	-12.9059	0.33586	0.72558	-6.53681	6.75E-05	6.81E-04
17	5.42E-15	1.54818	-13.3508	0.33835	0.7146	-6.68289	3.96E-05	5.18E-04
17.5	4.40E-15	1.48968	-12.9444	0.19007	0.70462	-6.83151	5.24E-05	8.43E-04
18	6.86E-15	1.46027	-14.5383	0.40128	0.67575	-6.95989	7.79E-05	2.98E-04
18.5	6.86E-15	1.41869	-14.2519	0.34165	0.65787	-7.08156	9.69E-05	3.27E-04
19	9.06E-15	1.34013	-40.1444	0.25505	0.68218	-7.2498	1.82E-04	2.87E-03
20	5.00E-27	1.26685	-39.063	0.22283	0.65758	-7.47028	5.47E-04	5.64E-03
21	4.86E-27	1.22229	-39.127	0.29842	0.6098	-7.65726	7.92E-04	2.88E-03
22	9.61E-27	1.1824	-38.8621	0.2662	0.56773	-7.84299	1.04E-16	7.72E-04
23	9.22E-27	1.14065	-38.633	0.35945	0.5349	-8.01168	1.16E-16	4.44E-04
24	1.62E-26	1.09751	-38.635	4.52E-05	0.51158	-8.17522	1.93E-16	4.66E-04
25	2.33E-26	1.08131	-38.6951	2.98E-05	0.46532	-8.3431	2.64E-16	0.00258
26	2.52E-26	1.0268	-38.7327	3.72E-05	0.45836	-8.50064	3.47E-16	1.02E-04
27	2.85E-26	0.99673	-38.7751	4.12E-05	0.43909	-8.63956	4.43E-16	2.12E-04

$\chi_{T1} = \chi_S(\text{Total}) + \Delta\chi_1, \chi_{T2} = \chi_S(\text{Total}) + \Delta\chi_1 + \Delta\chi_2$

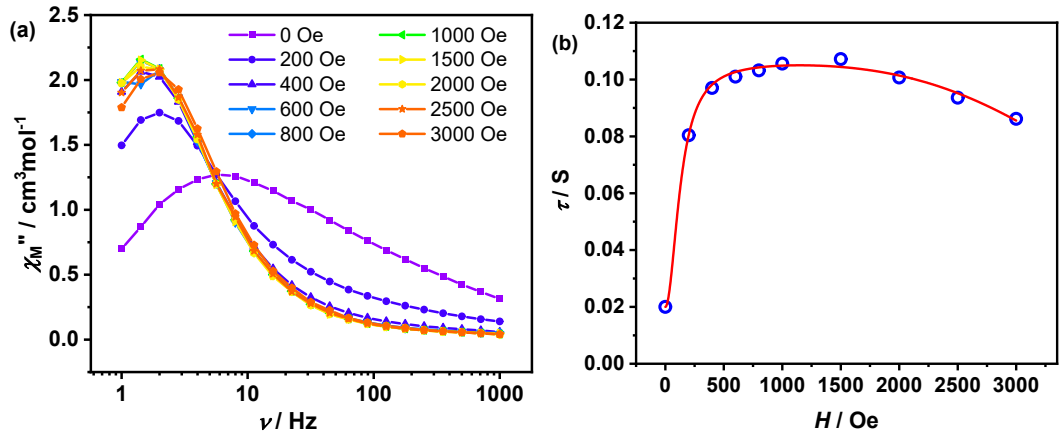

Fig. S10 (a) χ''_M vs. ν plot at 1.8 K in the frequency range of 1-1000 Hz under various applied dc for $\mathbf{Dy_xY_{2-x}}$. (b) Field-dependence of the relaxation time (blue circles) and the best fit curve (red line) for $\mathbf{Dy_xY_{2-x}}$.

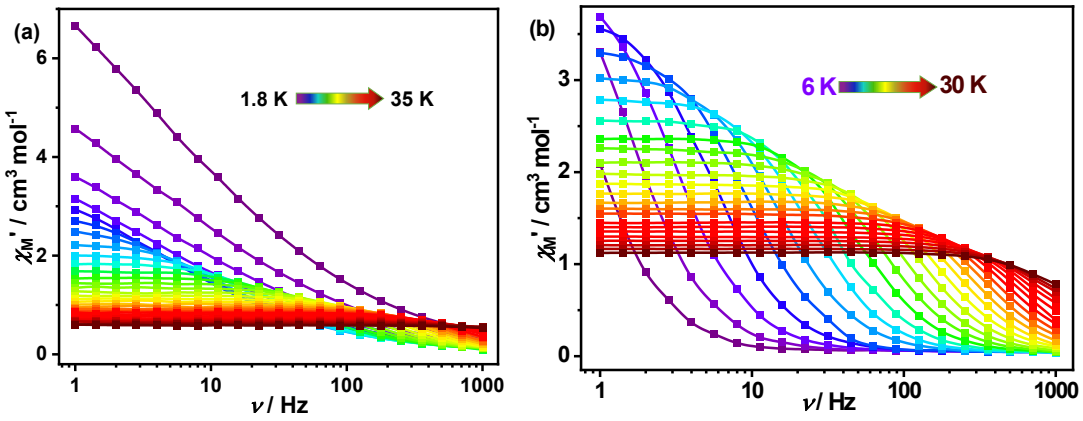

Fig. S11 Frequency-dependent of in-put phase (χ_M') ac susceptibilities under zero field (a) and under 1.5 kOe dc field (b) for $\mathbf{Dy_xY_{2-x}}$.

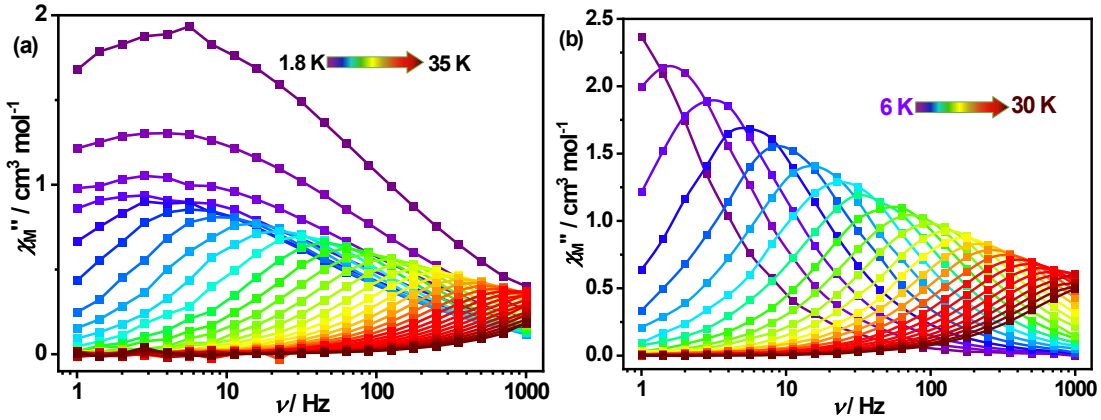

Fig. S12 Frequency-dependent of out-put phase (χ_M'') AC susceptibilities under zero field (a) and under 1.5 kOe dc field (b) for $\mathbf{Dy_xY_{2-x}}$.

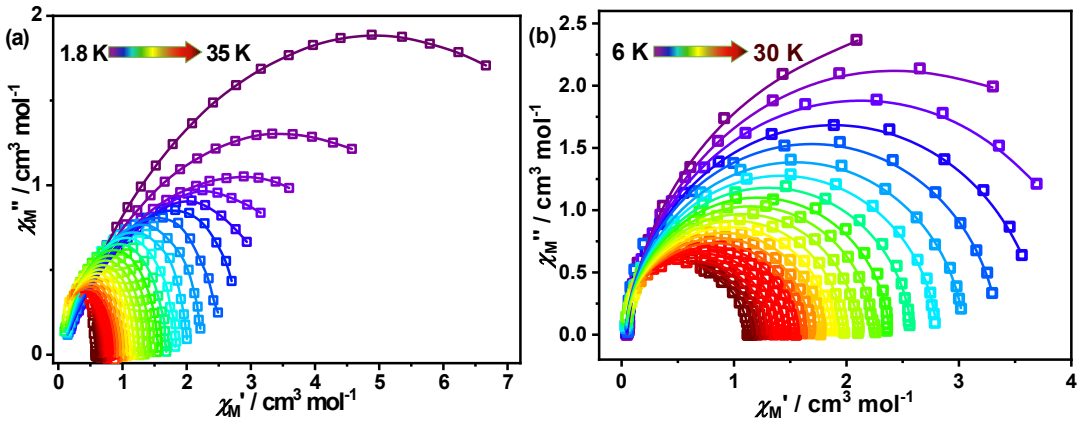

Fig. S13 Cole−Cole curves under zero DC-field (a) and under 1.5 kOe (b) for $\mathbf{Dy_xY_{2-x}}$. Solid lines represent the best fit with Debye model.

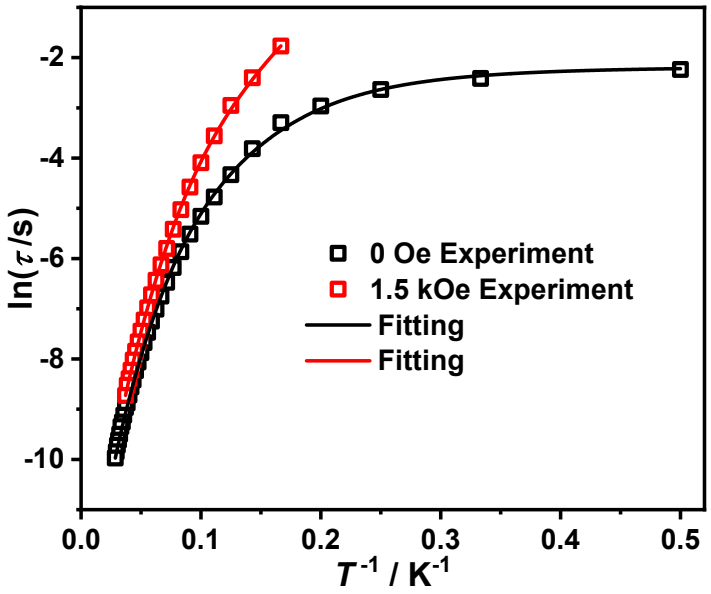

Fig. S14 Plot of ln(τ) versus T^{-1} under zero field (a) and under 1.5 kOe dc field (b) for **Dy_xY_{2-x}**.

Table S6 The best-fitted parameters obtained from the analyses of the Cole-Cole plots using the Debye model for **Dy_xY_{2-x}** under zero field.

T / K	χ_S(Total) / cm^3 mol^{-1}	$\Delta\chi$ / cm^3 mol^{-1}	ln(τ / s)	α	R^2
2	1.27E-08	9.52517	-2.23676	0.51406	0.03324
3	1.89E-08	6.66498	-2.41469	0.51973	0.02208
4	2.07E-08	5.38905	-2.63711	0.52318	0.00996
5	2.30E-08	4.71353	-2.964	0.51306	0.00468
6	3.05E-08	4.07911	-3.29513	0.48206	0.02933
7	2.57E-08	3.37327	-3.81284	0.42306	0.07014
8	1.08E-07	2.813	-4.33221	0.35771	0.11158
9	3.75E-07	2.4141	-4.77619	0.29969	0.10496
10	8.20E-07	2.12797	-5.15991	0.25411	0.08521
11	1.52E-06	1.91187	-5.51532	0.21763	0.0622
12	2.35E-06	1.72677	-5.86441	0.18242	0.04554
13	3.38E-06	1.58472	-6.17954	0.15863	0.03412
14	5.07E-06	1.46569	-6.47463	0.13943	0.02787
15	7.93E-06	1.36951	-6.74753	0.12586	2.03E-02
16	3.11E-02	1.26253	-7.00996	0.08812	0.01173
17	7.93E-02	1.19083	-7.24723	0.05093	0.00183
18	6.97E-02	1.1271	-7.46913	0.04904	0.00148
19	5.59E-02	1.07223	-7.67483	0.05237	2.15E-03
20	6.41E-02	1.01482	-7.87551	0.03882	0.00201
21	6.10E-02	0.96616	-8.06325	0.03631	2.20E-03
22	6.48E-02	0.92116	-8.23563	0.02744	0.00154
23	1.03E-01	0.87835	-8.41837	0.00565	4.47E-03

24	5.42E-02	0.84599	-8.55838	0.02975	0.00143
25	2.75E-02	0.81336	-8.71904	0.04094	0.00198
26	3.63E-02	0.78339	-8.87831	0.04016	0.00295
27	1.70E-12	0.75857	-8.96779	0.0434	0.00132
28	2.61E-12	0.73119	-9.12088	0.04512	0.00123
29	4.02E-12	0.70582	-9.25776	0.0419	9.09E-04
30	4.46E-12	0.67993	-9.34709	0.02072	0.00134
31	5.84E-12	0.663	-9.50092	0.04779	0.00134
32	9.60E-12	0.64221	-9.61578	0.02294	0.00282
33	1.14E-11	0.61961	-9.71696	0.02146	0.0016
34	1.77E-11	0.60487	-9.84768	0.01784	0.00221
35	2.61E-11	0.58767	-9.97155	4.45E-08	0.0025

$\chi_T = \chi_S(\text{Total}) + \Delta\chi$

Table S7 The best-fitted parameters obtained from the analyses of the Cole-Cole plots using the Debye model for $\mathbf{Dy_xY_{2-x}}$ under 1.5 Oe dc field.

T / K	χ_S(Total)/ cm^3 mol^{-1}	$\Delta\chi$ / cm^3 mol^{-1}	ln(τ / s)	α	R^2
6	0.05	5.43002	-1.77093	0.06207	0.0038
7	0.04486	4.7983	-2.40222	0.06295	0.00282
8	0.04477	4.20578	-2.95274	0.05445	0.00353
9	0.04292	3.72778	-3.55767	0.04742	0.00645
10	3.23E-02	3.3522	-4.09399	0.04068	0.01129
11	3.97E-02	3.04742	-4.57873	0.0422	0.00284
12	3.48E-02	2.80509	-5.02742	0.04157	0.00536
13	3.87E-02	2.5783	-5.41766	0.03617	0.00602
14	3.96E-02	2.38082	-5.80081	0.0284	0.00604
15	3.59E-02	2.2489	-6.12706	0.0344	0.00399
16	3.65E-02	2.1084	-6.43552	0.03206	0.00115
17	4.37E-02	1.97553	-6.7224	0.02456	0.00105
18	4.50E-02	1.8678	-6.98316	0.02382	0.00274
19	4.06E-02	1.7706	-7.2257	0.02432	8.82E-04
20	4.50E-02	1.67754	-7.44788	0.02085	0.00161
21	4.30E-02	1.60214	-7.65878	0.02533	0.00103
22	4.11E-02	1.54407	-7.84744	0.03103	0.00129
23	6.67E-02	1.45481	-8.02276	0.0105	9.31E-04
24	1.74E-02	1.40596	-8.22723	0.02959	0.00113
25	2.41E-02	1.35441	-8.39337	0.03486	7.26E-04
26	6.12E-02	1.29854	-8.52249	0.02546	0.00118
27	1.54E-15	1.25375	-8.72611	0.03362	8.19E-04

$\chi_T = \chi_S(\text{Total}) + \Delta\chi$

Details of *ab initio* calculations

For centrosymmetric binuclear **Dy_2**, the type two individual of Dy (III) fragments were calculated. Complete-active-space self-consistent field (CASSCF) calculations on individual Dy(III) fragments (recorded as Dy1 and Dy1a, as show in Figure S11) on the basis of single-crystal X-ray determined geometry have been carried out with MOLCAS 8.4 program package.[S1-S5] Each individual Dy(III) fragment was calculated keeping the experimentally determined structure while the other Dy(III) ion was replaced by diamagnetic Lu(III). The Calculated results are the same for fragments Dy1 and Dy1a, as shown in Table S8 and S9.

The basis sets for all atoms are atomic natural orbitals from the MOLCAS ANORCC library: ANO-RCC-VTZP for Dy(III); VDZP for close O; VDZ for distant atoms. The calculations employed the second order Douglas-Kroll-Hess Hamiltonian, where scalar relativistic contractions were taken into account in the basis set and the spin-orbit couplings were handled separately in the restricted active space state interaction (RASSI-SO) procedure. For individual Dy(III) fragment, active electrons in 7 active spaces include all *f* electrons (CAS(9 in 7)) in the CASSCF calculation. To exclude all the doubts, we calculated all the roots in the active space. We have mixed the maximum number of spin-free state which was possible with our hardware (all from 21 sextets, 128 from 224 quadruplets, 130 from 490 doublets). SINGLE_ANISO program was used to obtain the magnetic susceptibilities, energy levels, *g* tensors, m_J values, magnetic axes, *et al*., based on the above CASSCF/RASSI-SO calculations.[S2-S8]

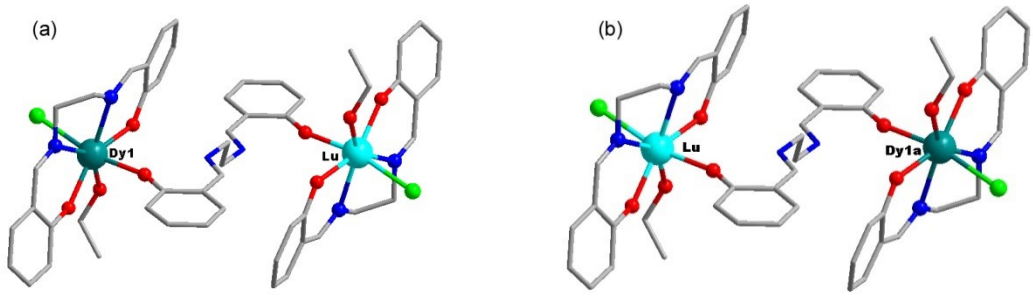

Fig. S15 Calculated Dy(III) fragment of **Dy_2**.

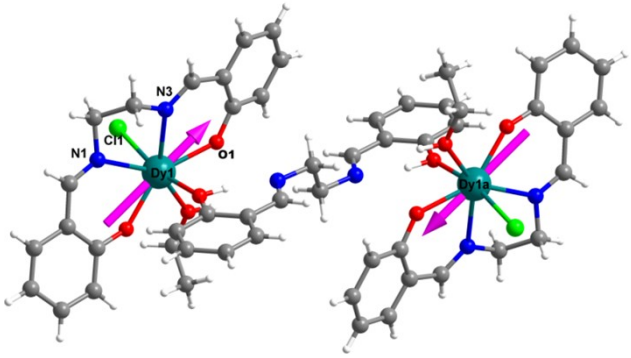

Fig. S16 The orientations of the anisotropy axes of the individual Dy(III) centres in **Dy_2**. Symmetry codes: a = 1 − *x*, − *y*, 1 – *z*.

Table S8 Calculated energy levels (cm^{-1}), g (g_x, g_y, g_z) tensors and m_J values of the lowest eight Kramers doublets (KDs) of individual fragments in **Dy_2**.

KDs	individual fragments Dy1and Dy1a in **Dy_2**		
	E /cm^{-1}	g	m_J
1	0.0	0.004 0.007 19.755	±15/2
2	291.7	0.082 0.104 16.863	±13/2
3	538.4	1.073 1.288 13.736	±11/2
4	674.7	4.397 6.104 9.055	±9/2
5	741.8	1.025 4.518 12.645	±3/2
6	810.3	0.275 1.667 14.450	±7/2
7	878.4	0.105 2.253 15.793	±1/2
8	904.5	0.700 2.264 17.193	±5/2

Table S9 Wave functions with definite projection of the total moment $|m_J>$ for the lowest two Kramers doublets (KDs) of individual fragments Dy1 and Dy1a in **Dy_2**.

	E /cm^{-1}	wave functions
Dy1, Dy1a	0.0	97.6%|±15/2>
	291.7	95.8%|±13/2>+2.8%|±9/2>

Table S10 Exchange energies E (cm^{-1}), the energy differences between each exchange doublets Δ_t (cm^{-1}) and the main values of the g_z for the lowest two exchange doublets of **Dy_2**.

	E	Δ_t	g_z
1	0.0	1.0×10^{-7}	0.034

2	0.449	3.8×10^{-8}	39.521

To fit the exchange interaction of **Dy_2**, two steps were adopted to obtain parameters. Firstly, we calculated the individual Dy(III) fragment using CASSCF/RASSI-SO to obtain the corresponding magnetic properties. Then, the exchange interaction between the magnetic centres is considered within the Lines model, while the account of the dipole-dipole magnetic interaction is treated exactly.[S9] The Lines model is effective and has been widely used in the research field of *d* and *f*-elements single-molecule magnets.[S10,S11]

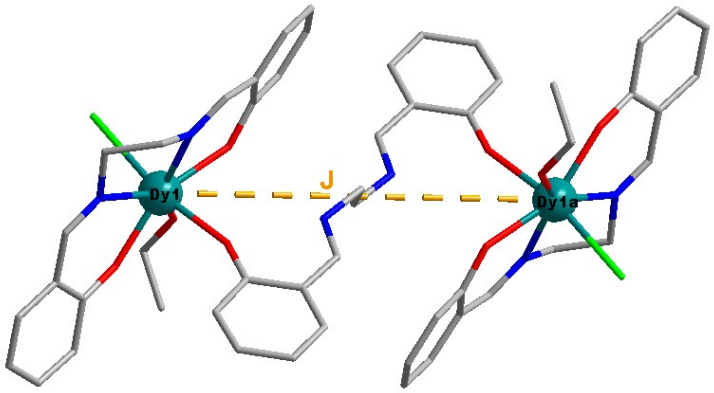

Fig. S17 Scheme of the Dy^{III}…Dy^{III} magnetic couplings in **Dy_2**. Symmetry codes: a = $1-x, -y, 1-z$.

The Ising exchange Hamiltonians for **Dy_2** is as shown in equation (1). Total coupling constants J_{total} that include dipole–dipole interaction (J_{dip}) and exchange coupling parameters (J_{exch}), as shown in equation (2). The dipole–dipole interaction (J_{dip}) is calculated with equation (3).

$$\hat{H}_{exch} = -J_{total}\hat{S}_{Dy1}\hat{S}_{Dy1a} \quad (1)$$

$$J_{total} = J_{dip} + J_{exch} \quad (2)$$

$$J_{dip} = -\frac{\mu_B^2 g_{1Z} g_{2Z}}{r^3}(\cos\theta - 3\cos\varphi_1\cos\varphi_2) \quad (3)$$

where θ is the angle between the main anisotropy axes on both Dy sites; φ_1 is the angle between the main magnetic axis on site 1 (Dy1) with the unit vector connecting the two Dy sites (n_{12}); φ_2 is the angle between the main magnetic axis on site 2 (Dy1a) with the unit vector connecting the two Dy sites (n_{12}); g_{1Z} is the Z component of the ground g tensor on site 1; g_{2Z} is the Z component of the ground g tensor on site 2; μ_B^2 is a constant (= 0.4329701512063995) in units of cm^{-1}/Tesla; r is the distance between the Dy1 and Dy1a, in Angstrom.

The parameters of calculation results are $\theta = 0$, $\varphi_1 = \varphi_2 = 47.923°$, $g_{1Z} = g_{2Z} = 19.75536463$, $r = 10.4636$ Å, $J_{dip} = -0.022$ cm^{-1}.

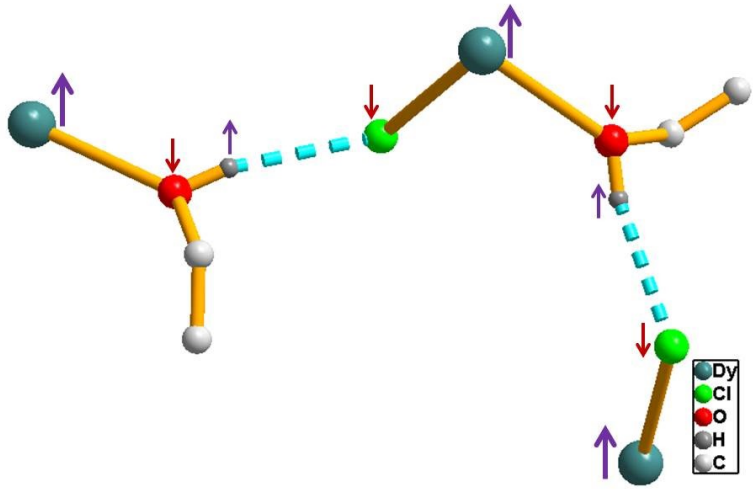

Fig S18 Schematic diagram of the spin-polarization mechanism between two Dy^{III} centres of neighbouring molecules through hydrogen bonding.

References

S1 F. Aquilante, J. Autschbach, R. K. Carlson, L. F. Chibotaru, M. G. Delcey, L. De Vico, I. F. Galván, N. Ferré, L. M. Frutos, L. Gagliardi, M. Garavelli, A. Giussani, C. E. Hoyer, G. Li Manni, H. Lischka, D. Ma, P. Å. Malmqvist, T. Müller, A. Nenov, M. Olivucci, T. B. Pedersen, D. Peng, F. Plasser, B. Pritchard, M. Reiher, I. Rivalta, I. Schapiro, J. Segarra-Martí, M. Stenrup, D. G. Truhlar, L. Ungur, A. Valentini, S. Vancoillie, V. Veryazov, V. P. Vysotskiy, O. Weingart, F. Zapata, and R. Lindh, *J. Comput. Chem.*, 2016, 37, 506-541.

S2 L. F. Chibotaru, *Struc. Bonding* (Berlin, Ger.) 2014, 164, 185-230.

S3 U. Liviu and L. F. Chibotaru, *Inorg. Chem.*, 2016, 55, 10043-10056; J. J. Baldoví, Y. Duan, R. Morales, A. Gaita-Ariño, E. Ruiz and E. Coronado, *Chem. Eur. J.*, 2016, 22, 13532-13539.

S4 U. Liviu and L. F. Chibotaru, *Phys. Chem. Chem. Phys.*, 2011, 13, 20086- 20090.

S5 L. F. Chibotaru and L. Ungur, *J. Chem. Phys.*, 2012, 137, 064112 (1-22).

S6 L. F. Chibotaru, L. Ungur and A. Soncini, *Angew. Chem. Int. Ed.*, 2008, 47, 4126- 4129.

S7 L. Ungur, W. Vanden Heuvel and L. F. Chibotaru, *New J. Chem.*, 2009, 33, 1224-1230.

S8 L. F. Chibotaru, L. Ungur, C. Aronica, H. Elmoll, G. Pilet and D. Luneau, *J. Am. Chem. Soc.*, 2008, 130, 12445- 12455.

S9 M. E. Lines, *J. Chem. Phys.*, 1971, 55, 2977-2984.

S10 K. C. Mondal, A. Sundt, Y. H. Lan, G. E. Kostakis, O. Waldmann, L. Ungur, L. F. Chibotaru, C. E. Anson and A. K. Powell, *Angew. Chem. Int. Ed.* 2012, 51, 7550-7554.

S11 S. K. Langley, D. P. Wielechowski, V. Vieru, N. F. Chilton, B. Moubaraki, B. F. Abrahams, L. F. Chibotaru and K. S. Murray, *Angew. Chem. Int. Ed.*, 2013, 52, 12014-12019.